PHYSICAL REVIEW B **82**, 201408(R) (2010)

Spontaneous symmetry breaking and Lifshitz transition in bilayer graphene

Y. Lemonik,[1] I. L. Aleiner,[1,2] C. Toke,[3] and V. I. Fal'ko[2,3]
[1]*Physics Department, Columbia University, New York, New York 10027, USA*
[2]*Kavli Institute for Theoretical Physics China, CAS, Beijing 100190, China*
[3]*Physics Department, Lancaster University, Lancaster LA1 4YB, United Kingdom*
(Received 3 November 2010; published 17 November 2010)

We derive the renormalization-group equations describing all the short-range interactions in bilayer graphene allowed by symmetry, the long-range Coulomb interaction, and band-structure parameters. For certain range of parameters, we predict the first-order phase transition to the uniaxially deformed gapless state accompanied by the change in the topology of the electron spectrum.

DOI: 10.1103/PhysRevB.82.201408 PACS number(s): 73.22.Pr, 73.21.−b

The Lifshitz transition (LiTr) (Ref. 1) is the simplest topological effect in the physics of metals. Its essence is the change in connectivity of isoenergetic surfaces, either as a function of electron density or external parameters, such as strain. As the change in the topology of the, e.g., Fermi surface cannot be continuous, all the observables in the system should experience singularities at the LiTr [also known as a half-integer-order phase transition (PT)]. Alternatively, the reconstruction of the Fermi surface may occur via an underlaying spontaneous symmetry breaking PT. The observation of the LiTr in the bulk metals is an extremely challenging task: a variation in the Fermi level in metals requires doping which introduces disorder and obscures the transition, whereas the application of strain requires high-pressure experiments.

The bilayer graphene (BLG) is a potentially ideal system to study the LiTr.[2] Unlike in conventional metals, electron density in BLG can be tuned by a gate voltage and high-quality suspended BLG devices have been fabricated.[3,4] The gapless low-energy electronic structure of the conduction and valence bands near the Brillouin-zone (BZ) corners in Bernal stacked BLG has a parabolic dispersion $\epsilon_{\pm} \approx \pm p^2/2m$ at intermediate energies determined by the intralayer and interlayer hops between closest neighbors. The electronic wave functions accumulate a $\phi=2\pi$, Berry phase as the momentum goes around a loop encompassing $p=0$. This causes the double degeneracy, $d_0=2$ (per one spin and one valley) of the zero-energy Landau level in magnetic fields.

These features, however, are not protected by the crystal symmetry. The parabolic dispersion is trigonally deformed at the lowest energies due to the next-neighbor interlayer hopping and the $\epsilon=0$ state splits into four Dirac points: one in the BZ corner and three offsets separated by momentum $2mv_3$ in Fig. 1(a) (this separation is about 0.1% of the size of BZ). The Dirac point in the BZ corner carries $\phi=-\pi$ and each of the offsets $\phi=\pi$ so that the total ϕ is conserved. This leads to $d_0=4$.

The central question of this Rapid Communication is the stability of the LiTr described above against the effect of the electron-electron interaction. There are two options: (i) the interaction does not break the C_{6v} symmetry of the crystal; this leads to a quantitative renormalization of the band-structure affecting, e.g., the density $n_{\mathrm{LiTr}}=(2/\pi^2)(mv_3/\hbar)^2$ corresponding to the LiTr; (ii) the interaction does break the symmetry leading to a qualitative transformation of the spectrum—the number of the Dirac points is then determined by the reduced symmetry (contradicting scenarios were suggested in Refs. 5–7). Using the renormalization-group (RG) treatment of the problem we found that: (i) n_{LiTr} is not renormalized; (ii) the most likely spontaneous symmetry breaking in BLG occurs by the generation of the asymmetric hopping in the effective Hamiltonian[5] with the same $\mathcal{C}_{2v}$ symmetry as a perturbation due to an $A-\tilde{B}$ sublattice displacement, see Fig. 1(b). For the gedanken experiment where v_3 is varied in the BLG at zero density, the symmetry breaking occurs via a first-order quantum PT after which the spectrum remains gapless but two Dirac points are annihilated and two other persist and carry $\phi=\pi$. For a more feasible experiment with a varying carrier density, n, the $\mathcal{C}_{6v}\rightarrow\mathcal{C}_{2v}$ transition may occur at $n=n_c$ whose relation to n_{LiTr} depends on microscopic parameters. If $n_c>n_{\mathrm{LiTr}}$, further decrease in $|n|$ will be followed by another LiTr in the $\mathcal{C}_{2v}$ phase illustrated in Fig. 1(b). The difference between the phases would manifest it-

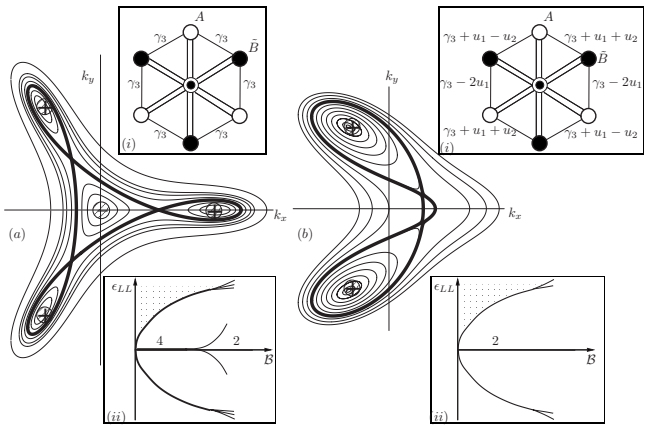

FIG. 1. Constant energy lines for the one-particle spectrum in the BLG. LiTr as a function of density occurs when the Fermi-level intersects the separatrix (bold line) for (a) unbroken $\mathcal{C}_{6v}$ symmetry of the graphene lattice; (b) symmetry breaking $\mathcal{C}_{6v}\rightarrow\mathcal{C}_{2v}$. Circles mark Dirac points and $\pm$ indicates Berry phases, $\phi=\pm\pi$. Insets show the tight-binding cartoons for the band structure (i) and the schematic evolutions of the Landau levels in the magnetic field and (ii) the number indicates the degeneracy per one spin and valley, d_0.

self through the persistence of different filling factors in Shubnikov-de Haas measurements into low magnetic fields ($\hbar eB/mc < mv_3^2$): $\nu = \pm 8(4)$ for $\mathcal{C}_{6v}(\mathcal{C}_{2v})$ phases.

The low-energy model for the bilayer graphene is formulated in terms of the states close to K and K' points of the Brillouin zone.[2] The Hamiltonian is

$$\hat{\mathcal{H}} = \int d^2\mathbf{r}\Psi_\sigma^\dagger[\hat{h}_0 + \hat{h}_w + \hat{h}_c + \hat{h}_{sr}]\Psi_\sigma. \tag{1a}$$

Hereinafter, the summation over repeated spin indices $\sigma = \pm 1/2$ is implied. A four component fermionic field $\Psi_\sigma = (\hat{\psi}_\sigma^{A,K}, \hat{\psi}_\sigma^{\tilde{B},K}; \hat{\psi}_\sigma^{\tilde{B},K'}, -\hat{\psi}_\sigma^{A,K'})$ lives in the valley (KK') and the sublattice ($A\tilde{B}$) spaces[2] (sublattices A and $\tilde{B}$ belong to the different layers). All matrices acting in this four-dimensional space are represented as direct products of the Pauli matrices $\hat{\tau}_i^{A\tilde{B}}, \hat{\tau}_i^{KK'}$, (i=0,1,2,3),

$$\hat{M}_i^j \equiv \hat{\tau}_i^{KK'} \otimes \hat{\tau}_j^{A\tilde{B}} \tag{1b}$$

and $\hat{\tau}_0^{\cdot\cdot}$ is the unit 2×2 matrix.

The kinetic energy is given by ($\hbar = 1, k_{x,y} = -i\partial_{x,y}$),

$$\hat{h}_0(k_{x,y}) = -[\hat{M}_3^1(k_x^2 - k_y^2) - 2\hat{M}_3^2 k_x k_y]/(2m). \tag{1c}$$

Together with Eq. (1c), the trigonal warping term,

$$\hat{h}_w(k_{x,y}) = v_3[\hat{M}_0^1 k_x + \hat{M}_0^2 k_y] \tag{1d}$$

determines the spectrum in Fig. 1(a).

The long-range Coulomb interaction

$$\hat{h}_c = \frac{e^2}{2}\int \frac{d^2\mathbf{r}'\Psi_{\sigma'}^\dagger(\mathbf{r}')\Psi_{\sigma'}(\mathbf{r}')}{|\mathbf{r}-\mathbf{r}'|} \tag{1e}$$

is the strongest in the system. However, due to the screening it does not scale and therefore, does not describe any symmetry breaking by itself. The latter is captured by the scaling of the marginal short-range interactions

$$\hat{h}_{sr} = (2\pi/m)\sum_{i,j=0}^{3} g_i^j \hat{M}_i^j[\Psi^\dagger \hat{M}_i^j \Psi]. \tag{1f}$$

The couplings g_i^j are not independent.[8] The $\mathcal{C}_{6v}$ symmetry of the bilayer constrains

$$g_1^1 = g_2^2 = g_1^2 = g_2^1 = g_G; \quad g_3^1 = g_3^2 = g_{E_2},$$

$$g_1^3 = g_2^3 = g_{E_2''}; \quad g_0^1 = g_0^2 = g_{E_1}; \quad g_1^0 = g_2^0 = g_{E_2''},$$

$$g_0^3 = g_{A_2}; \quad g_3^0 = g_{B_2}; \quad g_3^3 = g_{B_1}; \quad g_0^0 = g_{A_1}, \tag{1g}$$

where subscripts indicate the irreducible representations of the extended point group, see, e.g., Sec. III of Ref. 9. For example, E_2 is two-dimensional representation which does not change sign under C_2 rotation and describes the symmetry breaking shown on Fig. 1(b) whereas B_1 is the one-dimensional representation describing the breaking of the interlayer symmetry, $\mathcal{C}_{6v} \to \mathcal{C}_{3v}$.

The RG study of the model Eq. (1) is based on the analysis of diagrams shown in Fig. 2. The Coulomb interaction is

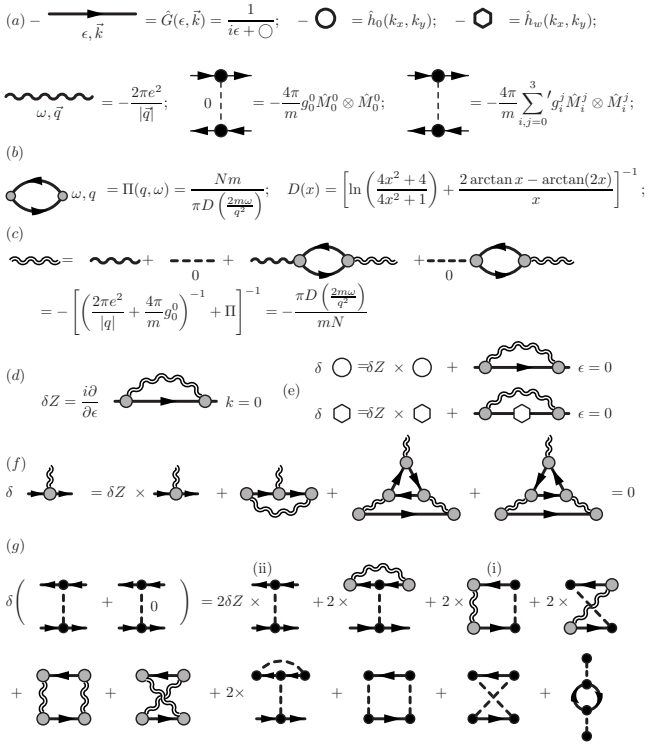

FIG. 2. Derivation of the RG equations. (a) Definitions of the elements; (b) polarization operator; (c) screening of the Coulomb interaction; [(d) and (e)] renormalization of one-particle spectrum; (f) gauge invariance of the scalar vertex; and (g) renormalization of the short-range interaction.

apparently the most relevant operator—its perturbative treatment leads to linear rather than logarithmic divergences. The screening of this interaction, see Fig. 2(c), makes it marginal; its value is $\simeq 1/[N\Pi(q,\omega)]$, where Π is the polarization operator. The formal justification for the approximation Fig. 2(c) is the $1/N$ expansion, which we believe is applicable for $N=4$ and the long-wavelength limit. Note, that g_0^0 enters together with the Coulomb interaction potential so that it drops out, see Fig. 2(c), and does not contribute to the running of the coupling constants. Other constants g_i^j are assumed to be small and treated in a first loop approximation.[10]

Because the polarization operator does not have logarithmic divergences and all of the interactions are considered in the first loop, the details of the cut-off scheme are not important. On each step we will restrict the internal momentum of the loop as $\mathcal{E} - d\mathcal{E} < k^2/2m(\mathcal{E}) \le \mathcal{E}$. We, then, rescale $\psi \to (1+\delta Z/2)\psi$, [$\delta Z$ is defined on Fig. 2(d)] to keep the term $\partial_\tau \psi$ in the Matsubara equation intact. As a bonus, the scalar vertex is also not renormalized for the reason of gauge invariance, see Fig. 2(f). Renormalizations of m and v_3, see Fig. 2(e), are given by[11]

$$d\ln m/d\ell = -d\ln v_3/d\ell = -\alpha_1/N; \quad \alpha_1 \approx -.078, \tag{2a}$$

where $\ell \equiv \log(\mathcal{E}_0/\mathcal{E})$ and $\mathcal{E}_0 \simeq 0.3$ eV limits the applicability of the two-band model of bilayer graphene.

The possible symmetry breakings are described by the scaling of the short-range interaction terms[11]

$$\frac{dg_i^j}{d\ell} = -\frac{\tilde{\alpha}\delta(E_2)_i^j}{N^2} - \frac{\alpha_1 g_i^j}{N} - NB_i^j(g_i^j)^2 - \sum_{k,l,m,n=0}^{3} C_{i;km}^{j;ln}\tilde{g}_k^l\tilde{g}_m^n\tilde{g}_i^j$$

$$\equiv g_i^j(1-\delta_{i0}\delta_{j0}) + \delta_{i0}\delta_{j0}\alpha_2/(2N), \alpha_2 \approx .469, \qquad (2b)$$

where $\tilde{\alpha}=\alpha_3-\alpha_2^2/16, \alpha_3\approx .066$, the symbol $\delta(E_2)_i^j$ is defined as $\delta(E_2)_{i=3}^{j=1,2}=1$ and $\delta(E_2)_i^j=0$ otherwise. The summation over repeated indices is not implied in Eq. (2b). The constants in Eq. (2b) are given by

$$B_i^j = \frac{1}{16}\sum_{l=1,2}\mathrm{tr}\{[\hat{M}_i^j,\hat{M}_3^l]^2\};$$

$$C_{i;km}^{j;ln} = \frac{1}{32}\{\mathrm{tr}[\hat{M}_i^j[\hat{M}_k^l,\hat{M}_m^n]]\}^2$$

$$+\frac{1}{64}\sum_{r=1,2}\{\mathrm{tr}\hat{M}_3^r(\hat{M}_k^l\hat{M}_i^j\hat{M}_m^n+\hat{M}_m^n\hat{M}_i^j\hat{M}_k^l)\}^2$$

$$+\frac{\delta_{ik}\delta_{jl}}{4}\sum_{r=1,2}\mathrm{tr}\{\hat{M}_m^n\hat{M}_3^r[\hat{M}_i^j,\hat{M}_3^r]\hat{M}_m^n\hat{M}_i^j\}. \qquad (2c)$$

Note that Eqs. (2b) and (2c) respect symmetry in Eq. (1g).

Equation (1f) is the main technical result of this Rapid Communication. They describe the evolution of all the band-structure parameters and all short-range interactions terms allowed by symmetry in the leading logarithmic approximation. To compare with the existing literature: the RG treatment of Ref. 5 considers only two possible terms (g_{E_2} and g_{A_2}), treats the Coulomb interaction as short range and neglects the warping in the spectrum; mean-field treatment of Refs. 6 and 7 corresponds to taking into account only one[6] [(i) of Fig. 2(g)] or two[7] diagrams [(i) and (ii) of Fig. 2(g)], without justification, and the subsequent projection on the B_1 representation.

RG flow and nonbroken symmetry. The density of electrons (or holes) at which the topology of the Fermi-surface changes is found from Eqs. (1c) and (1d) as $n_{\mathrm{LiTr}}=(2/\pi^2)(mv_3/\hbar)^2\simeq 2\times 10^{10}\mathrm{cm}^{-2}$ (estimated with $m=0.035$ and $v_3=v_3\simeq 10^7$ cm/s). According to Eq. (2a), the Coulomb part of the interaction does not renormalize n_{LiTr} but affects the energy of the saddle points in the single-particle spectrum $\mathcal{E}_{\mathrm{LiTr}}\equiv mv_3^2/2$. The bare value of this energy can be estimated using the bilayer parameters m, v_3 quoted above as $\mathcal{E}_{\mathrm{LiTr}}\simeq 1$ meV. The renormalized value is $\tilde{\mathcal{E}}_{\mathrm{LiTr}}=\mathcal{E}_{\mathrm{LiTr}}(\mathcal{E}_0/\mathcal{E}_{\mathrm{LiTr}})^{\alpha_1/N}\simeq\mathcal{E}_{\mathrm{LiTr}}(\mathcal{E}_{\mathrm{LiTr}}/\mathcal{E}_0)^{0.02}$, such a change is not observable.

RG flow and symmetry-breaking PT. The divergence of a coupling constant $g_\circ$ during the renormalization signals the symmetry breaking with the order parameter from the corresponding irreducible representation (a more complete classification, involving the magnetic and gauge symmetries will be reported elsewhere[12]).

Let us assume that the short-range interactions on the energy scale E_0 are negligible, $g_i^j=0$. The constant term in Eq. (2b) means that this point is not fixed and couplings g_{E_2} and g_{A_2} [see Eq. (1g)] will flow away from this point. Ignoring g_{A_2}, we obtain an equation for g_{E_2}

$$\frac{dg_{E_2}}{d\ell} = -\frac{c_1}{N(N+2)} - 2(N+2)(g_{E_2}-c_2)^2,$$

$$c_1 \approx \left[\frac{\alpha_3(N+2)}{N} - \frac{(\alpha_2-\alpha_1)^2}{8N}\right]; \quad c_2 \approx \frac{\alpha_2-\alpha_1}{4N(N+2)}. \qquad (3)$$

Note that $c_1>0$, for $N>0$, and no fixed-point exists; though α_3 appears small, its neglecting would lead to a nontrivial fixed point $g_{E_2}\simeq 1/N^3$. Solution of Eq. (3) is

$$g_{E_2}(\ell) = c_2 - \sqrt{\frac{c_1}{2N(N+2)^2}}\cot\left[\sqrt{\frac{2c_1}{N}}(\ell_0-\ell)\right], \qquad (4)$$

where ℓ_0 is found from $g_{E_2}(\ell=0)=0$. For $N=4$ we obtained $\ell_0\sim 7.1$. Inclusion of g_{A_2} shifts the pole slightly so that $(g_{E_2};g_{A_2})\propto(\ell_0-\ell)^{-1}(-1.67;0.85)$.

This divergence implies a symmetry breaking at $\mathcal{E}_{E_2}\simeq E_0 e^{-7.1}\simeq 0.3$ meV.[13] It is important to notice that $\mathcal{E}_{E_2}$ and $\mathcal{E}_{\mathrm{LiTr}}$ turn out to be of the same order and, therefore, have to be considered together. A more accurate theoretical comparison of those two energy scales requires more detailed knowledge about the microscopic values of the initial interaction constants which is not available at this time. Therefore, we will discuss the possible PTs for an arbitrary value of $\Upsilon\equiv\mathcal{E}_{E_2}/\mathcal{E}_{\mathrm{LiTr}}$.

If $\Upsilon\ll 1$, the divergence of g_{E_2} is terminated and the symmetry is not broken. A divergence of the coupling constant g_{E_2} at $\Upsilon\gtrsim 1$ indicates the symmetry breaking and appearance of the anomalous averages comprising the irreducible representation E_2 of the group $\mathcal{C}_{6v}$,

$$u_j = (2\pi/m)\langle\Psi_\sigma^\dagger\hat{M}_3^j\Psi_\sigma\rangle; \quad j=1,2. \qquad (5)$$

For studying the PT we have to consider the Landau free-energy density. It must be of the form

$$f = n_{\mathrm{LiTr}}\mathcal{E}_{\mathrm{LiTr}}\mathcal{F}_\Upsilon\left(\frac{u_1^2+u_2^2}{\mathcal{E}_{\mathrm{LiTr}}^2};\frac{u_1^3-3u_1u_2^2}{\mathcal{E}_{\mathrm{LiTr}}^3}\right) \qquad (6)$$

for the symmetry and dimensionality reasons. At $\Upsilon<\Upsilon_c$ (here $\Upsilon_c\simeq 1$), function $\mathcal{F}(x,0)$ has a local minimum at $x=0$ which at $\Upsilon>\Upsilon_c$, turns to a maximum. The presence of the cubic invariant prescribed by $\mathcal{C}_{6v}$ symmetry signals that the zero-temperature PT, under varying Υ, can be only of the first order and occurs at $\Upsilon<\Upsilon_c$.

Now, we argue that the value of the order parameter in the ordered phase is such that the electron spectrum has two Dirac points, as in Fig. 1(b). In the mean-field approximation, the one-particle Hamiltonian reads

$$\hat{H} = \hat{h}_0(k_{x,y}) + \hat{h}_w(k_{x,y}) - u_1\hat{M}_3^1 - u_2\hat{M}_3^2. \qquad (7)$$

At $u_1=-\mathcal{E}_{\mathrm{LiTr}}, u_2=0$ two Dirac points collide and disappear and the band structure of Fig. 1(b) is formed. At $u_1=3\mathcal{E}_{\mathrm{LiTr}}, u_2=0$ three Dirac points collide, and, once again, the spectrum with two Dirac points is formed.

The mean-field energy density is given by

$$f_{MF}(u_1,u_2) = (\Upsilon_c - \Upsilon)\frac{mu_iu_i}{2\pi} + \int \frac{d^2k}{\pi^2}\left[\epsilon(\mathbf{k}) - \epsilon(\mathbf{k})|_{u_{1,2}=0} - \frac{u_iu_j}{2}\frac{\partial^2\epsilon(\mathbf{k})}{\partial u_i\,\partial u_j}\bigg|_{u_{1,2}=0}\right], \quad (8)$$

where ϵ is the negative eigenvalue of $\hat{H}$, see Eq. (7), and the summation over the repeated indices $i,j=1,2$ is implied. The curvature of the energy density found from Eq. (8), see Fig. 3, indicates that indeed u_1 formed during the PT transforms the spectrum of Fig. 1(a) to that of Fig. 1(b).

The corrections to the mean-field cannot remove the singularity for the colliding Dirac points, as Hamiltonian (7) at low energies is protected by symmetry. Therefore, our conclusion about the number of Dirac points in the phases is more general than the mean-field derivation.

The first-order quantum PT has important consequences for the finite temperature phase diagram of BLG, see Fig. 3(c). At low temperatures $T \ll \mathcal{E}_{\mathrm{LiTr}}$, the PT remains of the first order up to some tricritical T_t and at $T > T_t$ the PT is continuous and belongs to three-states Potts model universality class.[5] The quantum PT can be studied as the function of density n controlled by the gate voltage and the phase diagram is on Fig. 3(d).

In conclusion, we investigated the interplay of the trigonal symmetry of the bare spectrum of the bilayer graphene with the electron-electron interaction. The derived RG equations allowed us to reveal the phase diagram[12] determined by the few (currently unknown) microscopic inputs. For a reasonably wide range of the initial conditions[13] we found $\mathcal{C}_{6v} \to \mathcal{C}_{2v}$ symmetry breaking and connected it with the change in the topology of the single-particle spectrum. We predicted the quantum phase transition of the first order as a function of the electron density. Such a PT may follow LiTr in the $\mathcal{C}_{6v}$ phase or precede the LiTr in the $\mathcal{C}_{2v}$ phase and it should be most readily observed in the hysteretic dependence of the conductivity on the gate controlled carrier density in the vicinity of the BLG neutrality point.

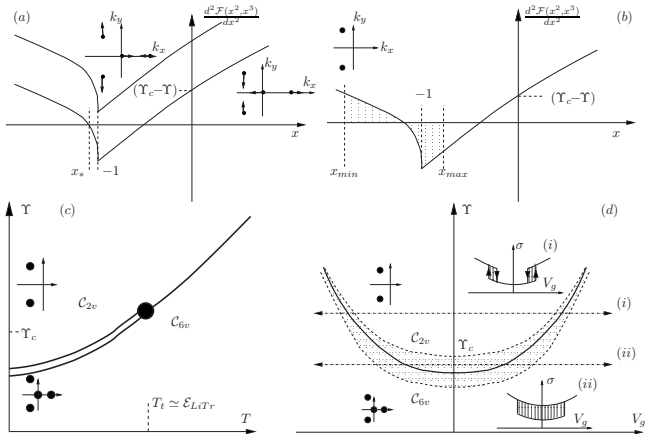

FIG. 3. [(a) and (b)] The curvature of the mean-field energy along the steepest decent direction. The square-root singularity is caused by the collision of the Dirac points shown on the inset. At $\Upsilon < \Upsilon_1 < \Upsilon_c$ extra local minimum and maximum are formed (a), such as $|u_1^{\max}| > \mathcal{E}_{\mathrm{LiTr}}$ (b), i.e., only two Dirac points remain. The total dashed area equals to zero. [(c) and (d)] The schematic phase diagrams for the finite temperature (c) and for quantum (d) (controlled by the gate voltage V_g) PTs. The insets show predicted hysteretic (or slow noise) behavior (dashed areas) of the conductivity for the corresponding paths on the phase diagram.

This work was supported by U.S. DOE under Contract No. DE-AC02-06CH11357 (Y.L. and I.A.), and by EPSRC under Grant Nos. EP/G041954 and oEP/G035954 and Royal Society Grant No. WM100048 (V.F.). We are grateful to A. Geim, K. Novoselov, and A. Chubukov for valuable discussions.

[1] I. M. Lishitz, Zh. Eksp. Teor. Fiz. **38**, 1565 (1960) [Sov. Phys. JETP **11**, 1130 (1960)]; A. A. Abrikosov, *Fundamentals of the Theory of Metals* (Elsevier, New York, 1988).

[2] E. McCann and V. I. Fal'ko, Phys. Rev. Lett. **96**, 086805 (2006).

[3] B. E. Feldman, J. Martin, and A. Yacoby, Nat. Phys. **5**, 889 (2009).

[4] A. Geim (private communication).

[5] O. Vafek and K. Yang, Phys. Rev. B **81**, 041401(R) (2010); A similar "nematic phase" was discussed in K. Sun, H. Yao, E. Fradkin, and S. A. Kivelson, Phys. Rev. Lett. **103**, 046811 (2009) for $\mathcal{C}_4$ and Kagome lattices.

[6] R. Nandkishore and L. Levitov, arXiv:0907.5395v1 (unpublished).

[7] R. Nandkishore and L. Levitov, Phys. Rev. Lett. **104**, 156803 (2010).

[8] I. L. Aleiner, D. E. Kharzeev, and A. M. Tsvelik, Phys. Rev. B **76**, 195415 (2007).

[9] D. M. Basko, Phys. Rev. B **78**, 125418 (2008).

[10] For similar treatment in monolayer see Ref. 8, J. E. Drut and D. T. Son, Phys. Rev. B **77**, 075115 (2008).

[11] The function $D(x)$ of Fig. 2(b) determines coefficients as $(\alpha_1;\alpha_2;\alpha_3) = \frac{1}{2\pi}\int_{-\infty}^{\infty}\frac{dxD(x)}{(1+x^2)^2}\left(\frac{1-3x^2}{(1+x^2)};2;\frac{D(x)}{4}\right)$.

[12] Y. Lemonik, I. L. Aleiner, and V. I. Fal'ko (unpublished).

[13] Line Eq. (4) is an unstable solution of Eq. (2b) and may be used only if the bare values of all other $g_\circ \lesssim 1/N$ so that they are still small at energy $\mathcal{E}_1$. All possible stable directions, their basins of attraction, and extremely rich phase diagram will be reported in Ref. 12.